XLIII CILAMCE
21–25, November, 2022
FOZ DO IGUAÇU – PR – BRAZIL

Numerical analysis of an unreinforced embankment on soft soil

Bianca C. Caetani[1], Naloan C. Sampa[1], Gustavo H. Rossi[1], Laura Z. Sassi[1]

[1]*Dept. of Civil Engineering, Federal University of Santa Catarina*
João Pio Duarte da Silva - 205, 88040-900, Santa Catarina, Brazil
bibicaetani@gmail.com, naloan.sampa@ufsc.br, gushenrirossi@hotmail.com, lazasassi@gmail.com

Abstract. The present work analyzed, through numerical modeling, the behavior of an unreinforced embankment on soft soil. The simulations were performed in the Abaqus software, from which the Mohr-Coulomb failure criterion was established for the granular material of the embankment and the Modified Cam Clay model for soft soils. As result, the paper presents and discusses the behavior of settlement, horizontal displacement, excess pore pressure, and effective stress variation as a function of time, horizontal distance, and depth. The adopted numerical model and the observed behavior patterns are satisfactory so that the results of this study can assist in the analysis of the performance of embankments on soft soils.

Keywords: soft soils, embankment, Abaqus, numerical model, performance.

1 Introduction

The rapid population growth combined with the expansion of urban centers and road-railway infrastructures increasingly drives the use of areas of saturated soft soil with high compressibility, low permeability and strength. As explained by Jesus et al. [1], the Brazilian coastal, including some areas of the State of Santa Catarina, is formed by thick deposits of compressible soft soils with low bearing capacity, responsible for the enormous challenges to the implementation of engineering works.

In these regions, due to the low bearing capacity and excessive settlement of the soft soils, large engineering works are usually not built directly on these soils, but rather on top of embankments. The execution of embankments aims to minimize future settlements and increase soil resistance over time due to the phenomenon of consolidation. In the case of embankments on very soft soils, other improvement techniques are commonly used to guarantee the stability of the embankment, reduce settlement or the execution time of works. According to Almeida and Marques [2], the choice of the most appropriate construction method depends on several factors, such as soil characteristics, the purpose of using the area, the neighborhood, deadlines, and construction costs.

Lambe and Whitman [3] state that the design of engineering works on soft soils demands the analysis of settlement, even in situations where the failure is not imminent, considering that settlement can lead a structure to collapse even if the safety factor against the shear failure of the foundation is high. The authors also cite 3 reasons for this analysis: the damage, utility, and appearance of the structure. Along the same line, Almeida and Marques [2] ensure that embankments on soft soils, with or without reinforcement, may fail through three different modes, named A, B, and C. In A, the failure occurs through the body of the embankment, not involving the soft clay layer. In B, the soft clay fails due to its low bearing capacity. In C, the failure is global and involves embankment and soft soil. For this reason, it is recommended to verify all failure modes, although the foundation instability (B) and global instability (C) modes are the main ones.

Based on the above statement, Limit Equilibrium Method and other analytical approaches are usually used to design and analyze the stability of embankments on soft soils. Despite its wide use, the Limit Equilibrium Method, according to Massad [4], considers the hypothesis of equilibrium in a soil mass, rigid-plastic, about to enter the sliding process. Thus, they are based on the equilibrium equations of horizontal forces and/or moments acting on the soil mass so they do not allow the analysis of the variation of stress, strain, and pore pressure within the soil mass. For more elaborate designs, it is common nowadays to employ not only the Limit Equilibrium

Method but also the Finite Element Method to assist in the stability and performance analysis of embankments on soft soils.

Because of this and considering the capability of the Finite Element Method, this paper analyzed, through numerical simulation in Abaqus software, the performance - the variation of excess pore pressure, effective stress, horizontal displacement and settlement - of an unreinforced embankment on soft soils.

2 Finite Element Model

A two-dimensional plane strain model was established to analyze the performance of the embankment on soft soil. The model consists of an embankment of granular material over a single layer of soft clay. The embankment has a height of 3.5 m, a total length of 20 m and a slope v:h equal to 1:2, while the soft soil layer has a total length of 60 m and a thickness of 10 m. This domain is large enough to avoid any significant boundary effects on calculated displacement, deformation and load. Due to symmetry, only one-half of the domain of the model was considered.

All domains have elements of the CPE8RP type (8-node plane strain quadrilateral element, biquadratic displacement, bilinear pore pressure and reduced integration). Figure 1 illustrates the mesh discretization of the finite elements, with greater refinements in regions with a tendency for stress and strain concentrations.

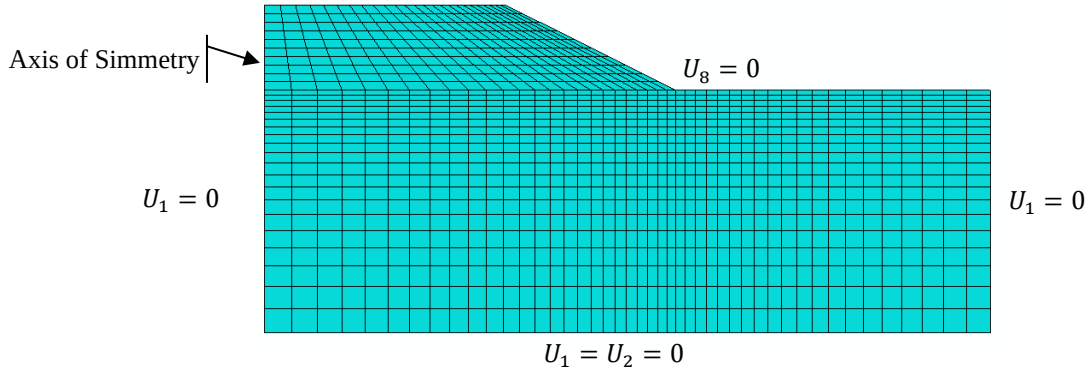

Figure 1. Representation of discretized finite element domain and boundary conditions

The three steps considered in the numerical modeling are geostatic, embankment execution, and consolidation. In the geostatic step, the initial stresses were generated in the soft soil layer using the Body Force option. The second step consisted of the execution of the embankment layer over a period of 1 month, considering the linear increment of load. Finally, the consolidation of the clay layer was monitored for 4 years after the completion of the embankment.

In the first step, 3 physical boundary conditions were defined. On the bottom side, both vertical (U_2) and horizontal (U_1) components of displacements were restricted. On the right-hand side, as well as on the symmetry axis, displacement was restricted only in the horizontal direction (U_1).

Regarding the permeability boundary condition, in the first step, the pore pressure is equal to 0 (U_8=0) on the top surface of the soft soil. At the beginning of the second step, the permeability boundary condition at the base of the embankment was deactivated, so that the pore pressure becomes zero at the crest and the embankment slope lines. This condition did not change until the end of the last step.

Seeking to represent the behavior of granular materials, the embankment was modeled as a homogeneous solid, obeying the Mohr-Coulomb failure criterion. The soft clay was considered saturated and modeled as a homogeneous solid with elastoplastic behavior, obeying the failure criterion of the Extended Modified Cam Clay model implemented in Abaqus.

The reference values of the parameters of both the embankment and soft clay materials were defined from the parameter range established based on the works of Han [5], Keykhosropur [6], Khabbazian [7], Elsawy [8], Alkhorshid [9], Yapage [10], Fang [11] and Almeida [12]. Table 1 presents the parameters of the embankment material while Tab. 2 summarizes the parameter of the soft soil.

Table 1. Parameters of the granular material of embankment

Parameter	Reference values	Variation range
Initial void ratio - e_0	0.65	-
Bulk unit weight - γ (kN/m³)	20	18 - 22
Cohesion - c (kN/m²)	2	0 - 5
Internal friccional angle - ϕ (º)	30	25 - 40
Dilatancy - ψ (º)	10	0 - 10
Elastic Module - E (kN/m²)	1000	500 - 80000
Poisson's ratio - ν	0.3	0.3 – 0.35
Permeability coefficient - k (m/s)	0.01	-

Table 2. Parameters of soft soil

Parameter	Reference values	Variation range
Initial void ratio - e_0	1,2	1 - 2
Bulk unit weight - γ (kN/m³)	15	14 - 18
Recompression index - κ	0,05	0.03 – 0.09
Poisson's ratio - ν	0.33	0.35 – 0.45
Compression index - λ	0.2	0.11 – 0.5
Slope of the critical state line - M	1	0.85 – 1.4
Initial size of the yield surface - p'/σ'_{v0}	37.5	-
Size of the yield surface in the wet side - β	1	-
Ratio of the flow stress - K	1	-
Permeability coefficient - k (m/s)	2.50E-08	-
Lateral earth pressure at rest - $K_0 = 1 - \text{sen}\,\phi$	0.58	0.58 – 0.66

For the analysis, the values of vertical displacement (settlement), horizontal displacement, pore pressure, and effective vertical stress were exported from Abaqus to Excel. Figure 2 shows 11 points, 3 horizontal lines and 7 vertical lines where the data were extracted. The data extracted in the points were used for analysis over time, while the information collected in the lines allows analysis along depth (vertical direction) or horizontal distance.

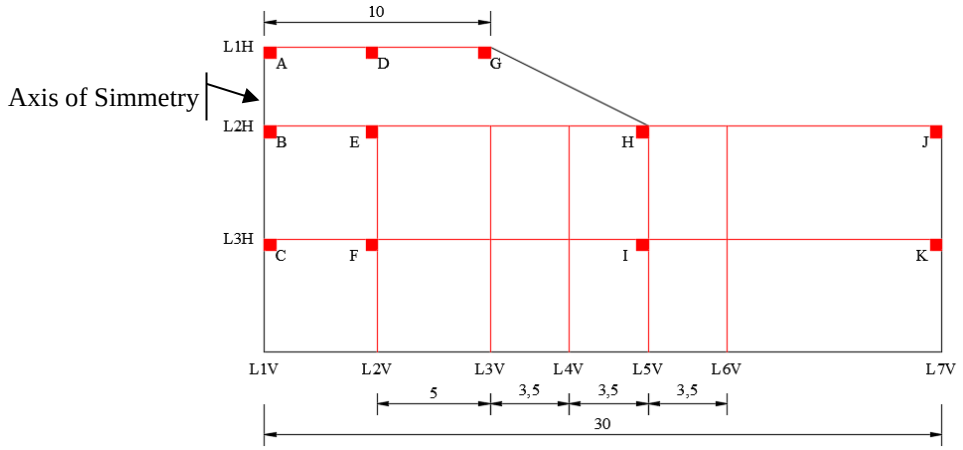

Figure 2. Points and lines used to extract the data

3 Results and Discussion

This section presents and discusses the analyses of settlement, horizontal displacement, excess pore pressure and effective vertical stress. The distribution of these variables throughout the model domain, at a given time, was analyzed from the images and data extracted from Abaqus. The following items present figures showing the variation of the variable's behavior as a function of time, depth, or horizontal distance.

3.1 Settlement Analysis

Figure 3 illustrates the variation of settlement, in meters, at the end of the last step (4 years). The maximum settlement is equal to 35 cm and it occurred at the top of the embankment, while the maximum soil lift observed near the toe of the embankment is around 2 cm.

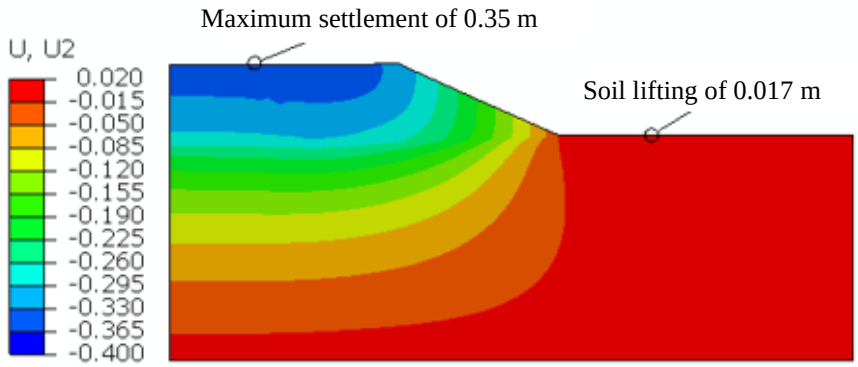

Figure 3. Variation of the settlement – 4 years

Figure 4a shows the variation of settlement as a function of time for points A, B, D, E, and G. The highest normalized settlement (3.5% or 35cm) occurred at points A and D, located at the top of the embankment. On the other hand, the maximum settlement of the soft soil layer (points B and E) was approximately 28.6 cm.

During the construction period of the embankment, point H, located at the toe of the embankment, presented a positive settlement equal to 9 cm. Due to the large settlement of the soil below the central region of the embankment, the positive settlement decreases significantly after the completion of the embankment.

Figure 4b illustrates the variation of settlement along the horizontal distance for lines L1H (embankment surface) and L2H (soft soil surface). It is evident, based on the geometry of the embankment, that the closer to its symmetry axis, the greater the settlement. It is also noted that the average settlement of the clay layer is approximately 16 cm in 1 month and 29 cm in 4 years. Clearly, Fig 4b shows the soil uplift at the foot of the embankment during the loading stage (1 month) and its return to the initial state as the clay layer consolidation advances.

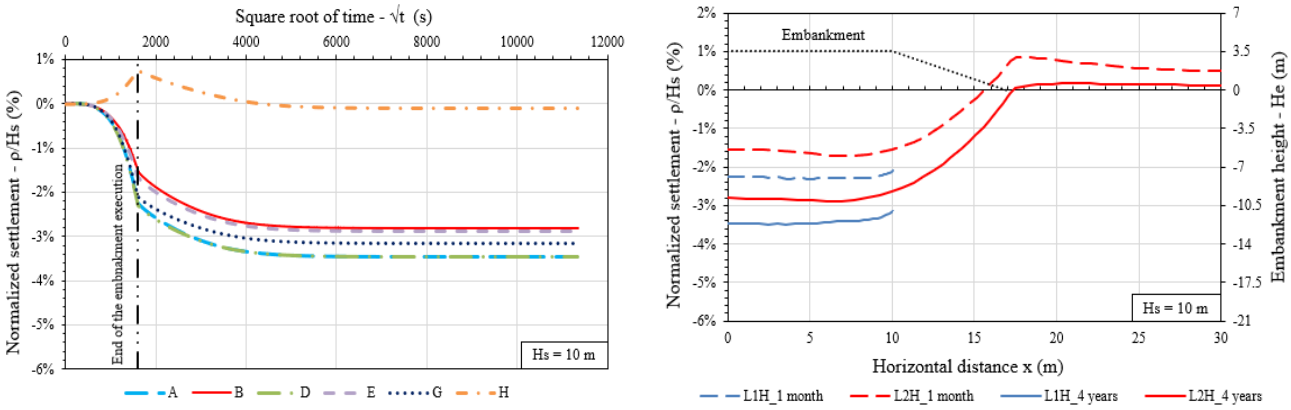

Figure 4. Variation of the settlement – a) versus time, b) versus horizontal distance

The embankment surface (L1H) undergoes an average settlement of approximately 23 cm and 34.5 cm in 1 month and 4 years, respectively. It is worth noting that the settlement in 4 years is almost equal to that of the 12.9th month after completion of the embankment, the beginning of settlement stabilization. The maximum difference in settlement on the embankment surface (L1H) is 1.5 cm at 1 month, and 3.1 cm at 4 years, values lower than the maximum recommended by DNIT [13] for embankments classified as II and III.

3.2 Horizontal displacement Analysis

The monitoring of horizontal displacement of both embankment slopes and foundation soils is extremely important in the stability analysis of embankments on soft soils since significant horizontal displacement indicates the rapid formation of failure surface and the possibility of instability.

Considering the times of 1 month and 4 years, Fig. 5 shows the variation of the horizontal displacement along the following vertical lines: L2V, L3V, L4V, L5V and L6V. As expected, the horizontal displacement reduces with depth in all lines. For a given depth, the horizontal displacements increase in the following order: L2V, L6V, L3V, L5V and L4V. L3V, L5V and L4V are located below the embankment slope, where the highest concentration of horizontal displacements occurs.

Focusing only on the horizontal displacement of the extreme lines at 1 month, it is observed that the largest horizontal displacement in L2V was around 5.9 cm, while the largest value was approximately 18 cm in L4V. On the other hand, at the time of 4 years, the largest horizontal displacement in L2V and L4V regressed to near 4 cm and 13 cm, respectively.

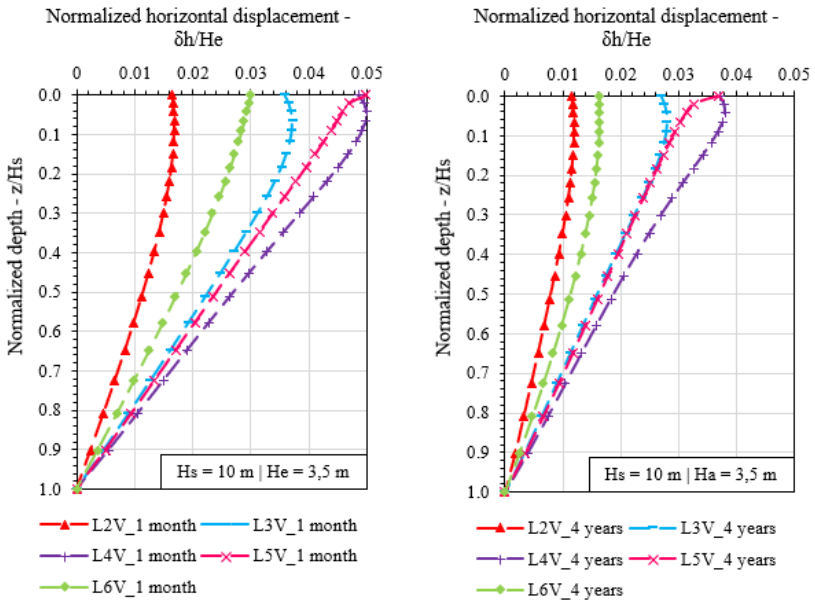

Figure 5. Variation of the horizontal displacement along the depth

3.3 Pore pressure Analysis

This section analyzes the performance of the embankment from the results of excess pore pressure as a function of horizontal distance and depth. As expected, the highest excess pore pressures are concentrated near the symmetry axis. In all soil domains, the excess pore pressure is practically zero from the 12th month after the completion of the embankment.

Figure 6a shows the variation of the excess pore pressure normalized by the effective vertical stress (q) of 35 kPa applied by the embankment on the ground surface. The normalized excess pore pressures in the middle of the layer are highest only in the first month, and decrease as one moves away from the axis of symmetry. Considering the time of 1 month, for example, it is observed that 80% of the stress applied by the embankment is transformed into excess pore pressure in the soil domain near the symmetry axis. On the other hand, as mentioned earlier for the times of 1 year and 4 years, the excess pore pressure is practically null.

The analysis of the variation of excess pore pressure along the depth was performed for the lines L1V (axis of symmetry), L2V (5 m away from the axis of symmetry) and L5V (at the foot of the embankment), considering the time of 1 month, as shown in Fig 6b. In all cases, the excess pore pressure increases along the depth, varying from zero to a maximum value that depends on the position of the line under analysis. In other words, the normalized excess pore pressure tends to remain constant at greater normalized depths, however, these depths increase as the line moves away from the axis of symmetry. The average values of the normalized excess pore

pressure at greater depths are approximately equal to 0.31, 0.78 and 0.82 for lines L5V, L2V and L1V, respectively.

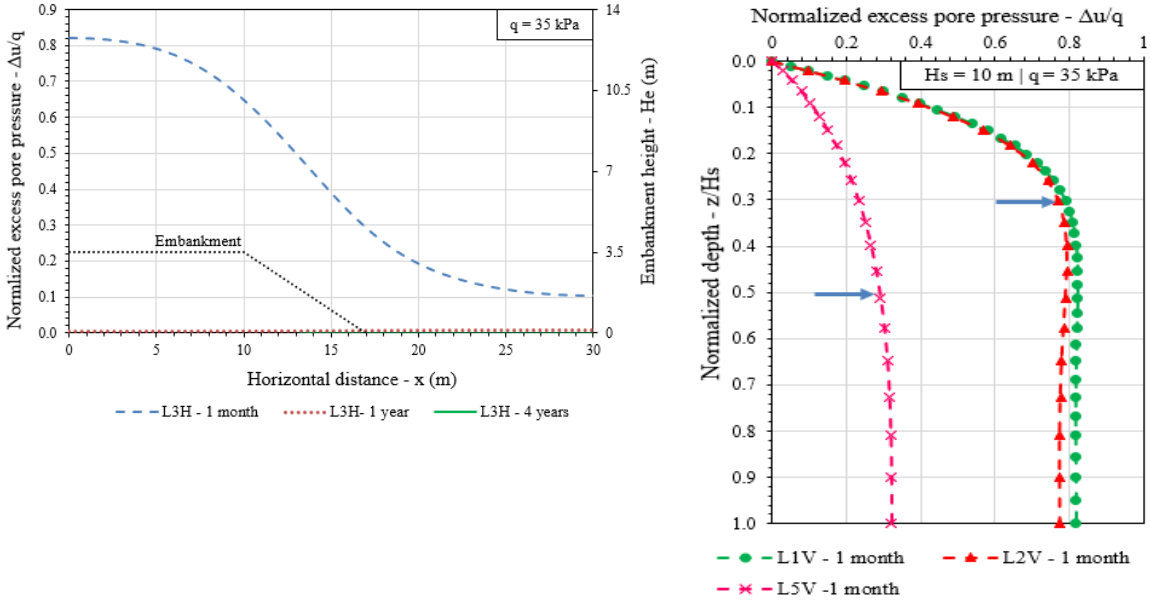

Figure 6. Variation of excess pore pressure versus – a) horizontal distance, b) normalized depth

3.4 Increment of vertical stress Analysis

At the end of the embankment execution, effective stress of 35 kPa is applied to the soft soil surface. Considering the times of 1 month and 4 years, it is observed in Fig. 7 that the curves of lines L1V and L2V present similar behavior - the increment of effective vertical stress decreases with depth, as expected.

In 1 month, the increment of vertical stress varies from 2 kPa to 6 kPa at normalized depths greater than 0.4. However, in 4 years, after the total consolidation of the clay layer, there is a significant increase in the effective vertical stress along the depth in all lines. For example, in line L5V, there is an increase of effective vertical stress of approximately 10 kPa at the base of the clay layer. On the other hand, in lines L2V and L1V, the increment of vertical stress varies almost linearly from 35 kPa at the surface of the layer to 29 kPa at the base of the clay layer.

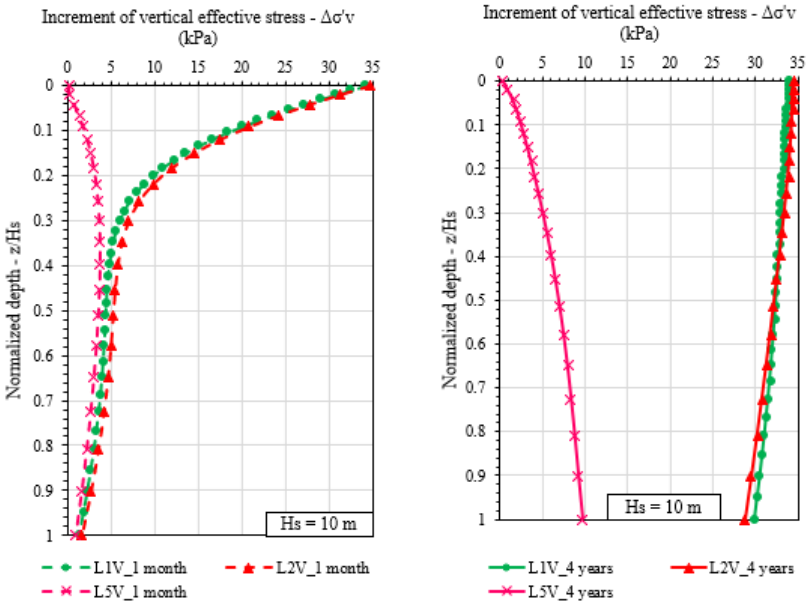

Figure 7. Variation of excess pore pressure – a) versus horizontal distance, b) normalized depth

4 Conclusions

The paper analyzes the behavior of an unreinforced embankment on soft soil by the Finite Element Method in the Abaqus software. The variation of the settlement, horizontal displacement, excess pore pressure and vertical stress increment along the depth, time and horizontal distance were presented and discussed.

During the execution of the embankment, two distinct behaviors were observed: lifting the soil near the foot of the embankment and settlement of the soil below it. Upon completion of the embankment, the soil below has undergone significant settlements while the soil near the foot has practically returned to its initial position due to the stabilization of the loading rate, while the settlement rate advances over time.

Significant horizontal displacements occurred on the slope and soil below, with the highest values found in the slope centerline. After the completion of the embankment, there was a reversal of the horizontal displacement over time until stabilization.

Regarding the excess pore pressures, the highest values were observed in the middle of the soil layer during the execution of the embankment and increased along the depth. Furthermore, these values decrease as one moves away from the axis of symmetry and also over time due the consolidation process. Finally, the results highlight the increase in the effective vertical stress during soil consolidation.

Understanding the variation of the settlement, horizontal displacement, excess pore pressure and increment of vertical stress along the depth, time and horizontal distance can assist in the analysis of the embankment's performance on soft soils.

Acknowledgments. The authors thank the Federal University of Santa Catarina for the infrastructure and financial support.

Authorship statement. The authors hereby confirm that they are the sole liable persons responsible for the authorship of this work, and that all material that has been herein included as part of the present paper is either the property (and authorship) of the authors, or has the permission of the owners to be included here.

References

[1] J. J. Jesus, B. C. Caetani, G. F. Costa, N. C. Sampa, D. C. Sanchez. “Soluções adaptadas para o reforço de fundações com estacas raiz”. In: *XX Congresso Brasileiro De Mecânica Dos Solos E Engenharia Geotécnica (COBRAMSEG*), Campinas, 2022.
[2] M. Almeida, M..E. S. Marques. *Aterros sobre solos moles: projeto e desempenh*o. Oficina de textos, São Paulo, 2014.
[3] T. W. Lambe, R. V. Whitman. *Soil mechanics*. John Wiley and Sons, Inc., New York, 1969.
[4] F. Maissad. *Obras de Terra: curso básico de geotecnia*. Oficina de Textos, 2. ed. São Paul, 2010.
[5] J. Han, M. A. Gabr. “Numerical Analysis of Geosynthetic-Reinforced and Pile-Supported Earth Platforms Over Soft Soil”. *Journal Geotechnical Geoenvironmental Engineering*. n. 128, p. 44-53, 2002.
[6] L. Keykhosropur, A. Soroush, R. Imam. “3D numerical analyses of geosynthetic encased stone columns”. *Geotextiles and Geomembranes*, n. 35, p. 61-68, 2012.
[7] M. Khabbazian, V. N. Kaliakin, C. L. Meehan. “3D Numerical Analyses of Geosynthetic Encased Stone Columns”. In *International Foundation Congress and Equipment Expo*, Orlando, Florida, 15 - 19 mar., 2009.
[8] M. B. D. Elsawy. “Behaviour of soft ground improved by conventional and geogrid-encased stone columns, based on FEM study”. *Geosynthetics International*, n. 4, p. 276–285, 2013.
[9] N. R. Alkhorshid, G. L. S. Araújo, E. M. Palmeira. “Geosynthetic Encased Column: comparison between numerical and experimental results. *Soils and Rocks”*, n. 44(4), 2021.
[10] N. N. S. Yapage, D. S. Liyanapathirana, H. G. Poulos, R. B. Kelly. “Numerical Modeling of Geotextile-Reinforced Embankments over Deep Cement Mixed Columns Incorporating Strain-Softening Behavior of Columns”. *International Journal of Geomechanics*. v. 15, n. 2, 2015.
[11] Z. Fang. Physical and Numerical Modelling of the Soft Soil Ground Improved by Deep Cement Mixing Method. 2006, Thesis (Doctor in Civil Engineering), The Hong Kong Polytechnic University, 2006.
[12] M. S. S. Almeida, I. Hosseinpour, M. Riccio. “Performance of a geosynthetic encased column (GEC) in soft ground: numerical and analytical studies”. Geosynthetics International, 20, n. 4, 252–262, 2013.
[13] Departamento Nacional de Infraestrutura de Transportes. DNIT 381/2021 – PRO: Projeto de aterros sobre solos moles para obras viárias. Brasília: Ed. Núcleo dos Transportes, 2021.